

The excited state absorption of  $\text{Er}^{3+}:\text{LiYF}_4$  and  $\text{Er}^{3+}:\text{Na}_5\text{Y}_9\text{F}_{32}$ 

C. Labbé, J.L. Doualan\*, S. Girard, P. Le Boulanger

*Lab. de Spectroscopie Atomique, UPRES A 6084, ISMRA, Bd. Maréchal Juin, 14050 Caen Cedex, France***Abstract**

The excited state absorption cross-sections in  $\pi$  and  $\sigma$  polarisations are obtained for the transition  ${}^4\text{I}_{13/2} \rightarrow {}^4\text{I}_{11/2}$  and  ${}^4\text{I}_{13/2} \rightarrow {}^4\text{I}_{9/2}$  in  $\text{Er}^{3+}:\text{LiYF}_4$ . The population ratio between the two excited states  ${}^4\text{I}_{11/2}$  and  ${}^4\text{I}_{13/2}$  in  $\text{Er}^{3+}:\text{LiYF}_4$  and  $\text{Er}^{3+}:\text{Na}_5\text{Y}_9\text{F}_{32}$  have been performed using the measured gain cross-sections in the range 2.6–3  $\mu\text{m}$ . The experiments have been done for two pump wavelengths—488 nm and 1.534  $\mu\text{m}$ . © 1998 Elsevier Science S.A.

*Keywords:* Excited state absorption; Gain cross-section; Erbium;  $\text{LiYF}_4$

**1. Introduction**

Solid-state laser materials with an emission around 3  $\mu\text{m}$  are interesting for medical applications because of the strong absorption of water at this wavelength. The  $\text{Er}^{3+}$  ion has been demonstrated to lase at room temperature in this domain in both oxide and fluoride crystals [1]. This emission operates on the transition from  ${}^4\text{I}_{11/2}$  to  ${}^4\text{I}_{13/2}$ . In the fluoride materials ( $\text{LiYF}_4$  also called YLF,  $\text{CaF}_2$ , etc.), the lifetimes of both levels are typically a few milliseconds due to the low rate of multiphonon relaxation. The self-terminated laser emission comes from the long lifetime of  ${}^4\text{I}_{13/2}$ . Under optical pumping, there is a distribution of the excited population between the two levels  ${}^4\text{I}_{11/2}$  and  ${}^4\text{I}_{13/2}$ . The relative populations between them depend on the pump wavelength, the pump intensity, the branching ratios and the upconversion process  ${}^4\text{I}_{13/2}$ ,  ${}^4\text{I}_{13/2} \rightarrow {}^4\text{I}_{15/2}$ ,  ${}^4\text{I}_{9/2}$ . The energy transfers between two neighbouring ions leading to an upconversion effect are usually complicated and therefore the distribution of the populations is relatively difficult to estimate [2]. The wavelength can also shift during the laser emission, and the position of the final emission wavelength could be difficult to deduce knowing only the upconversion coefficient and the efficiency of the pumping.

For that, in the present work, we have measured the average relative populations for these two levels using both excited state absorption and stimulated emission in the range 2.6–3  $\mu\text{m}$ . The results are obtained by a classical pump probe experiment. The gain cross-section is mea-

sured and the population ratio is deduced using calculated absorption and emission cross-sections. Dening et al. [3] have measured this ratio for a 2%  $\text{Er}^{3+}:\text{YLF}$  sample. We have extended it to other concentrations 1, 4.3 and 11.2% in YLF. We have also pumped the samples using successively two different wavelengths—488 nm and 1.534  $\mu\text{m}$ —to modify the relative populations for a given concentration. On the other hand, the absolute excited-state absorption cross-section of the transition  ${}^4\text{I}_{13/2} \rightarrow {}^4\text{I}_{9/2}$  was measured between 1.4 and 1.8  $\mu\text{m}$ . The gain cross-section of 5%  $\text{Er}^{3+}:\text{Na}_5\text{Y}_9\text{F}_{32}$  in the range 2.6–3  $\mu\text{m}$  has also been performed.

**2. Experimental methods**

Crystals doped with different  $\text{Er}^{3+}$  concentrations have been pulled with a home-made pulling apparatus using the Czochralsky technique. The final  $\text{Er}^{3+}$  concentrations have been determined on a reference crystal analysed by the inductively coupled plasma (ICP) technique. The absorption spectroscopy provides the ground-state absorption cross-sections and the relative concentration by comparing with the reference crystal analysed. The stimulated emission cross-section  $\sigma_{\text{SE}}$  from an excited state to the ground state can be obtained by the reciprocity method from the absorption  $\sigma_{\text{ABS}}$  [4] on the same transition:

$$\sigma_{\text{SE}}(\lambda) = \sigma_{\text{ABS}}(\lambda) \frac{Z_1}{Z_u} e\left[\left(\frac{E_{z1} - hc}{\lambda}\right)/kT\right] \quad (1)$$

where  $Z_1$  and  $Z_u$  are the partition functions, respectively of

\*Corresponding author. Tel.: +33 2 31452561; fax: +33 2 31452557.

the lower and the upper states,  $E_{z1}$  is the zero line of the transition. The emission cross-section can also be determined from the emission spectrum by the Fütchbauer–Ladenburg (F.L.) method [5]:

$$\sigma_{SE} = \frac{\lambda^5 \beta_R}{8\pi n^2 \tau_R} \frac{I(\lambda)}{\int \lambda I(\lambda) d\lambda} \quad (2)$$

where  $\beta_R$  and  $\tau_R$  are the branching ratio and the radiative lifetime respectively,  $I(\lambda)$  is the fluorescence emission spectrum. The difficulty is to know the exact values of  $\beta_R$  and  $\tau_R$ . But they can be estimated using the well known Judd–Ofelt (J.O.) analysis [6]. With Eq. (2), the cross-section has the correct shape but its magnitude could be only roughly estimated.

The excited-state absorption and stimulated emission cross-sections are measured by a pump probe technique at room temperature. The experimental device is similar to that used in Ref. [7]. A sample is excited by a pump beam, an Ar\* ion laser at 488 nm or a Colour Centre Laser (CCL) at 1.534  $\mu\text{m}$ . The pump beam is mechanically modulated at low frequency, around 10 Hz. A quartz diode lamp modulated at 1 kHz probes the sample alternatively with and without the pump. The wavelength selection is provided after the sample by a monochromator. Different detectors like PbS cells, InSb or InGaAs photodiodes, depending on the wavelength, measure the optical signal. For the polarised measurements a Glan Thompson polariser was used. But its transmission decreases because of the calcite absorption beyond 2.7  $\mu\text{m}$ . Therefore the S/N ratio becomes progressively worse when the wavelength increases in the infrared. In the experiment, a first lock-in amplifier synchronised on the probe modulation measures the mean transmission intensity  $I$  through the sample and a second lock-in amplifier measures the variation  $\Delta I$  of the transmission induced by the pump. The transmitted intensity when the pump is switched off is given by

$$I_u = I_0 e^{-\sigma_{GSA} N_T L} \quad (3)$$

where  $N_T$  is the total concentration of  $\text{Er}^{3+}$ ,  $L$  is the length of the sample and  $\sigma_{GSA}$  is the cross-section of the ground-state absorption (GSA). Whereas, when the pump is switch on, the expression becomes:

$$I_p = I_0 e^{(-\sigma_{GSA} N_1 + \sigma_{SE}^{(2)} N_2 - \sigma_{ESA}^{(2)} N_2 + \sigma_{SE}^{(3)} N_3 - \sigma_{ESA}^{(3)} N_3) L} \quad (4)$$

In this experiment, only the three first levels, namely  $^4I_{15/2}$ ,  $^4I_{13/2}$  and  $^4I_{11/2}$ , are supposed populated. Their concentrations are denoted  $N_1$ ,  $N_2$  and  $N_3$ , respectively, while  $\sigma_{SE}$  and  $\sigma_{ESA}$  are the cross-sections of the stimulated emission (SE) and of the excited-state absorption (ESA), respectively (the exponent is related to the level concerned). The ion concentrations respect the conservation rule:

$$N_T = N_1 + N_2 + N_3 \quad (5)$$

The relative variation  $\Delta I/I$  is reduced and therefore we can write

$$\begin{aligned} \frac{\Delta I}{I} &\approx A \ln \frac{I_p}{I_u} \\ &= A(\sigma_{GSA}(N_2 + N_3) + \sigma_{SE}^{(2)} N_2 - \sigma_{ESA}^{(2)} N_2 + \sigma_{SE}^{(3)} N_3 \\ &\quad - \sigma_{ESA}^{(3)} N_3) L \end{aligned} \quad (6)$$

where  $A$  is the calibration coefficient of the experiment. Usually the calibration is done in the part of the spectrum where the absorption cross-section is known and when only one excited state level is populated. For the fluoride crystals, the two metastable levels  $^4I_{13/2}$  and  $^4I_{11/2}$  can be significantly populated, therefore the calibration is more difficult. The following procedure was used. Around 2.7  $\mu\text{m}$ , the relative intensity given by Eq. (6) can be modified as:

$$\frac{\Delta I}{I} \approx A\{\beta \sigma_{SE}^{(3)} - (1 - \beta) \sigma_{ESA}^{(2)}\} (N_2 + N_3) L \quad (7)$$

where  $\beta$  is the ratio between the upper state and the total excited states population:

$$\beta = \frac{N_3}{(N_2 + N_3)} \quad (8)$$

$\sigma_{SE}$  is calculated by the F.L. equation (Eq. (2)),  $\sigma_{ESA}$  is deduced from  $\sigma_{SE}$  by the reciprocity method (Eq. (1)). The coefficients  $\beta$  and  $A(N_2 + N_3)L$  are adjusted to fit the measured spectrum. On the other hand in the 1.4–1.6- $\mu\text{m}$  range the only transition is  $^4I_{15/2} \leftrightarrow ^4I_{13/2}$  and the relative variation is given by:

$$\frac{\Delta I}{I} \approx A\{\sigma_{GSA} + (1 - \beta) \sigma_{SE}^{(2)}\} (N_2 + N_3) L \quad (9)$$

The coefficient  $\beta$  cannot be directly obtained with a satisfactory precision from Eq. (9) because  $\sigma_{ESA}$  and  $\sigma_{SE}$  are additive. In Eq. (9) the absorption measurement provides  $\sigma_{ESA}$ ,  $\sigma_{SE}$  is obtained by reciprocity (Eq. (1)),  $\beta$  comes from Eq. (7) and then the coefficient  $A(N_2 + N_3)L$  is obtained. Now it becomes easy to have the gain cross-section in the 2.6–3- $\mu\text{m}$  range:

$$\sigma_{\text{gain}} = \beta \sigma_{SE}^{(3)} - (1 - \beta) \sigma_{ESA}^{(2)} \approx \frac{\Delta I}{I} \frac{1}{A(N_2 + N_3) L} \quad (10)$$

### 3. Results

The ESA  $^4I_{13/2} \rightarrow ^4I_{9/2}$  is very close to the emission  $^4I_{13/2} \rightarrow ^4I_{15/2}$  (Fig. 1). The overlap of these two transitions can perturb the laser emission by excited-state absorption. The upconversion rate by resonant energy transfer depends on the overlap between the absorption and the emission spectra. The knowledge of the cross-section for this transition is necessary to calculate the upconversion coefficient using classical energy transfer models. For  $\text{Er}^{3+}:\text{YLF}$ , the shape has been measured [8] but not the

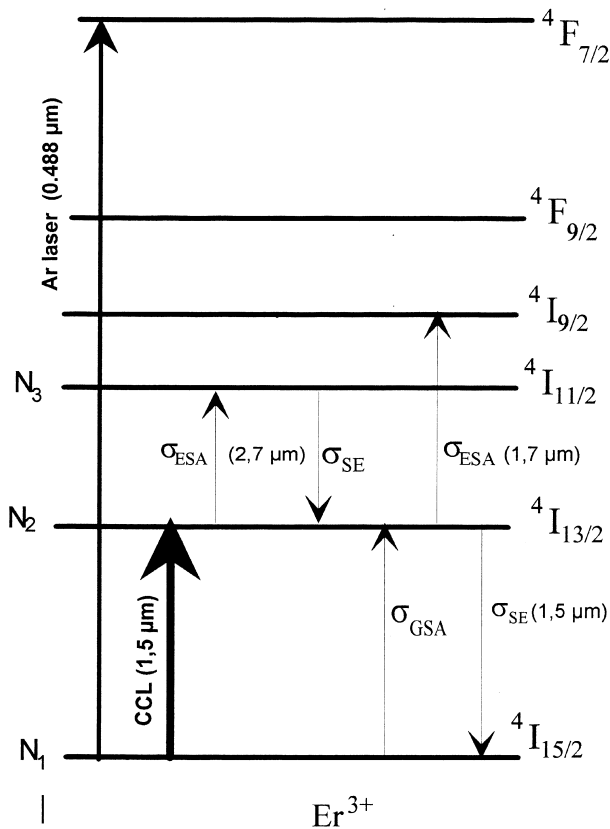


Fig. 1. The energy level scheme of the  $\text{Er}^{3+}$  ion.

absolute cross-section. To know its magnitude, it is necessary to have the  ${}^4\text{I}_{13/2}$  population density. In our experiments, the first step is to measure the population ratio. After that, the cross-section is deduced. They are measured for the two polarisations  $\sigma$  and  $\pi$  (Fig. 2). The overlap between ESA and SE cross-sections is very low and does not strongly affect a possible laser emission of the  ${}^4\text{I}_{13/2} \rightarrow {}^4\text{I}_{15/2}$  [9]. Because of this small overlap, the upconversion effect should be relatively small under the pump intensity used in our experiment. Therefore, a direct excitation into  ${}^4\text{I}_{13/2}$  using a CCL at  $1.534 \mu\text{m}$  provides an efficient excitation only in the first excited-state level. For a 1% doped crystal the upconversion has low efficiency and the population ratio is reduced to  $\beta=0.05$ . The ESA  ${}^4\text{I}_{11/2} \rightarrow {}^4\text{F}_{9/2}$  around  $1.8 \mu\text{m}$  is very low, whereas it is stronger for an 11.2% doped crystal. In this case, the population ratio becomes  $\beta=0.42$ .

The interesting laser transition in  $\text{Er}^{3+}$ -doped fluoride crystals is  ${}^4\text{I}_{11/2} \rightarrow {}^4\text{I}_{13/2}$ . The efficiency depends on the inversion population and the part of the stimulated emission compared to the absorption one. The wavelength dependence of the gain comes from the different cross-sections between Stark sublevels and the Boltzmann distribution across the Stark sublevels. After calibration, the experiment provides directly the gain cross-section versus the wavelength through Eq. (10) for a given pump intensity. It becomes possible to predict the wavelength

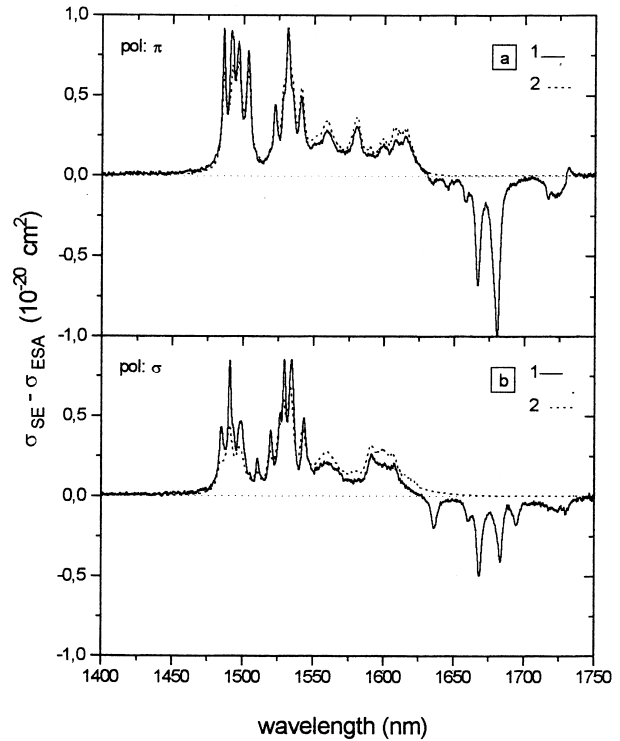


Fig. 2. The  $\pi$  (a) and  $\sigma$  (b) polarisation in  $\text{Er}^{3+}$ :YLF pumped at 488 nm: (1) the stimulated emission cross-section of  ${}^4\text{I}_{13/2} \rightarrow {}^4\text{I}_{15/2}$  and the excited-state absorption cross-sections of  ${}^4\text{I}_{13/2} \rightarrow {}^4\text{I}_{9/2}$  measured; (2) the stimulated emission cross-section of  ${}^4\text{I}_{13/2} \rightarrow {}^4\text{I}_{15/2}$  calculated by the reciprocity method.

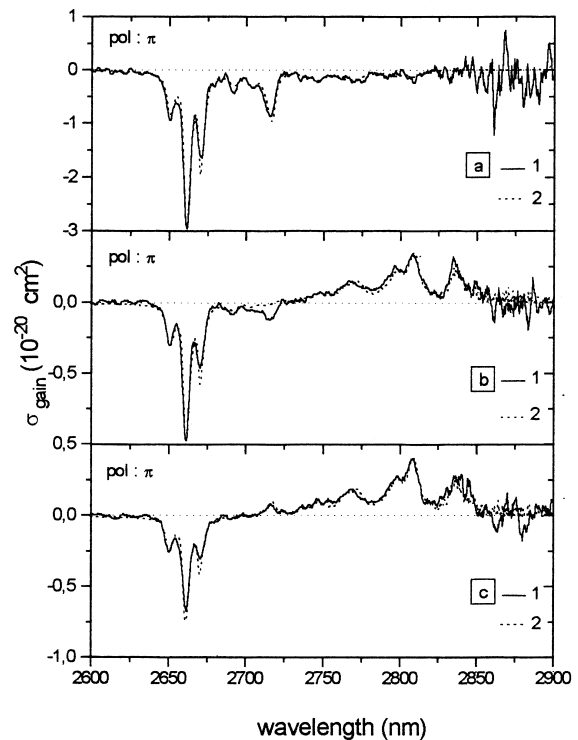


Fig. 3. The gain cross-sections measured (1) and calculated (2) of  ${}^4\text{I}_{13/2} \leftrightarrow {}^4\text{I}_{11/2}$  in  $\pi$  polarisation for the 1 (a), 4.3 (b) and 11.2% (c)  $\text{Er}^{3+}$ -doped YLF crystals pumped at 488 nm.

Table 1

The population ratio  $\beta$  of the 1, 4.3 and 11.2%  $\text{Er}^{3+}$ -doped YLF crystals and of the 5%  $\text{Er}^{3+}$ -doped  $\text{Na}_5\text{Y}_9\text{F}_{32}$

	$\beta$			
	1% $\text{Er}^{3+}$ :YLF	4.3% $\text{Er}^{3+}$ :YLF	11.2% $\text{Er}^{3+}$ :YLF	5% $\text{Er}^{3+}$ : $\text{Na}_5\text{Y}_9\text{F}_{32}$
Pol. $\pi$ (488 nm)	0.27	0.46	0.48	0.53
Pol. $\pi$ (1.534 $\mu\text{m}$ )	0.05	0.27	0.42	—

The measurement are in  $\pi$  polarisation for the two pump wavelengths 488 nm and 1.534  $\mu\text{m}$ .

where the laser emission is expected. The stimulated emission cross-section for the  $\pi$  polarisation is greater than for the  $\sigma$  polarisation, so this  $\pi$  polarisation will be systematically preferred for laser experiments. For the 1, 4.3 and 11.2%  $\text{Er}^{3+}$ -doped YLF crystals, the gain cross-section (Fig. 3) and the population ratio (Table 1) were measured. In the experiments, for all samples, the pump power was kept at 1.8 W for  $\lambda_p = 488$  nm and 300 mW for  $\lambda_p = 1.534$   $\mu\text{m}$ . In the population rate, the contribution part of the upconversion depends on the concentration ions and on the absorbed pump power. This process is quadratic with the absorbed pump power until saturation effects start to appear. From these spectra, the  $\sigma_{\text{ESA}}$  and  $\sigma_{\text{SE}}$  can be deduced (Fig. 4). The shape of these cross-sections fit well with the predicted one using the F.L. formula (Eq. (2)). To adjust the magnitude, it is necessary to choose a ratio  $\beta_R/\tau_R = 55 \text{ s}^{-1}$ . For a radiative lifetime  $\tau_R = 5.8$  ms, the branching ratio is  $\beta_R = 0.32$ .

In  $\text{Er}^{3+}$ :YLF the mean laser emission wavelength is at

2.81  $\mu\text{m}$  [10], it corresponds to the maximum of the  $\sigma_{\text{gain}}$  (Fig. 3). The stimulated emission cross-section at 2.81  $\mu\text{m}$   $\sigma_{\text{SE}} = 1.7 \cdot 10^{-20} \text{ cm}^2$  is close to the result obtained in Ref. [3] ( $\sigma_{\text{SE}} = 1.25 \cdot 10^{-20} \text{ cm}^2$ ). The other laser wavelengths for emissions are at 2.66, 2.716, 2.77, 2.84 and 2.85  $\mu\text{m}$  [11]. The emission at 2.66  $\mu\text{m}$  is possible only if the population inversion is very high. For the emission at 2.716  $\mu\text{m}$ , the ratio must be just greater than 0.5 and for the other wavelengths the ratio is lower.

In the 5%  $\text{Er}^{3+}$ -doped  $\text{Na}_5\text{Y}_9\text{F}_{32}$  pumped at 488 nm only the gain cross-section in the 2.6–3- $\mu\text{m}$  range was measured (Fig. 5b). The calibration was done with the emission spectra and Eq. (1) and Eq. (2) to provide the SE and ESA cross-sections (Fig. 5a). The population ratio was found equal to  $\beta = 0.53$ . The inversion population is more important than in YLF. One reason for that is the lifetime ratio defined by  $\tau_{11/2}/\tau_{13/2}$ , which is 0.48 for YLF and 0.77 for  $\text{Na}_5\text{Y}_9\text{F}_{32}$  [12]. The population inversion is greater in  $\text{Na}_5\text{Y}_9\text{F}_{32}$  but the cross-section is stronger in

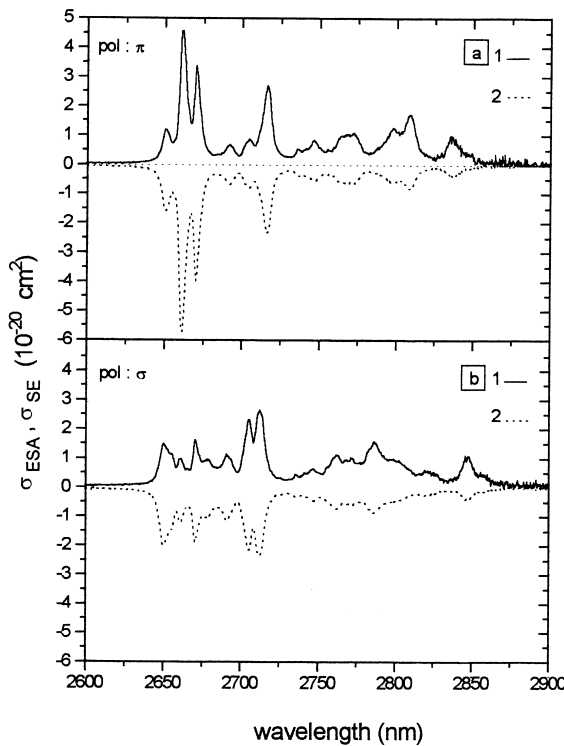


Fig. 4. The stimulated emission cross-section (1) of  ${}^4\text{I}_{11/2} \rightarrow {}^4\text{I}_{13/2}$  and the excited-state absorption cross-section (2) of  ${}^4\text{I}_{13/2} \rightarrow {}^4\text{I}_{11/2}$  for the  $\pi$  (a) and  $\sigma$  (b) polarisation in  $\text{Er}^{3+}$ :YLF pumped at 488 nm.

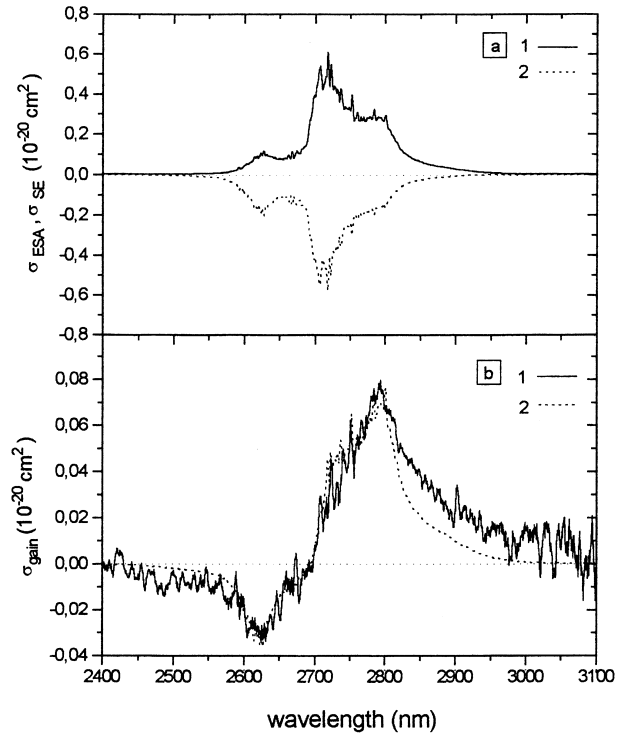


Fig. 5. In the 5%  $\text{Er}^{3+}$ -doped  $\text{Na}_5\text{Y}_9\text{F}_{32}$  pumped at 488 nm: (a) the stimulated emission cross-sections (1) of  ${}^4\text{I}_{11/2} \rightarrow {}^4\text{I}_{13/2}$  and the excited-state absorption cross-sections (2) of  ${}^4\text{I}_{13/2} \rightarrow {}^4\text{I}_{11/2}$ ; (b) the gain cross-sections measured (1) and calculated (2) of  ${}^4\text{I}_{13/2} \leftrightarrow {}^4\text{I}_{11/2}$ .

YLF due to the optical anisotropy of the material, to the relatively high odd component of the crystal field, and to the single site occupied by the rare earth. Finally, the gain cross-section is expected to be more favourable for laser emission around 2.8  $\mu\text{m}$  in YLF than in  $\text{Na}_3\text{Y}_9\text{F}_{32}$ .

## References

- [1] J.A. Caird, S.A. Payne, Paramagnetic Ion Lasers, in: M.J. Weber (Ed.), Handbook of Laser Science and Technology, Suppl. 1, Lasers, CRC, Boca Raton, FL, 1991, p. 3.
- [2] M. Pollnau, Th. Graf, J.E. Balmer, W. Lüthy, H.P. Weber, Phys. Rev. A 49(5) (1994) 3990.
- [3] A. Diening, T. Jensen, G. Huber, CLEO Europe, Hamburg, QWD10, Sept. 1996.
- [4] S.A. Payne, L.L. Chase, L.K. Smith, W.L. Kway, W.F. Krupke, IEEE J. Quantum Electronics 28(11) (1992) 2619.
- [5] B.F. Aull, H.P. Jenssen, IEEE J. Quantum Electronics 18(5) (1982) 925.
- [6] B.R. Judd, Phys. Rev. 127 (1962) 750; G.S. Ofelt, J. Chem. Phys. 37 (1962) 511.
- [7] J.L. Doualan, P. Le Boulanger, S. Girard, J. Margerie, F.S. Ermenoux, R. Moncorgé, ICL'96, Prague P2–56, J. Luminesc. (1997) (to be published).
- [8] J. Koetke, G. Huber, Appl. Phys. B 61 (1995) 151.
- [9] A.A. Kaminskii, Phys. Stat. Sol. (a) 148 (1995) 9.
- [10] M. Pollnau, R. Spring, Ch. Ghisler, S. Wittwer, W. Lüthy, H.P. Weber, IEEE J. Quantum Electronics 32(4) (1996) 657.
- [11] F. Auzel, S. Hubert, D. Meichemin, Appl. Phys. Lett. 54(8) (1989) 681.
- [12] C. Labbé, P. Le Boulanger, S. Girard, J. Margerie, J.Y. Gesland, TSSL, Wroclaw, Poland, Sept. 1996, p. 24.